Research Article

Journal of Environmental Nanotechnology

Comparative Study of Thermal Performance of Sinusoidal Wavy Corrugated Plate Heat Exchanger with MWCNT and CuO Nanoparticles in Water as Working Fluids

K. N. V. Sreedevi[1*] and Somanchi Naga Sarada[2]

[1]Department of Mechanical Engineering, Chaitanya Bharathi Institute of Technology (A), TG, India
[2]Department of Mechanical Engineering, JNTUH University College of Engineering, Science and Technology, Hyderabad, TG, India
Received: 25.01.2026 Accepted: 25.02.2026 Published: 30.03.2026
*knvsreedevi_mech@cbit.ac.in

ABSTRACT

Global energy demand necessitates improved efficacy of heat transfer process. Nanofluid is an innovative heat transfer fluid created by dispersing nanoparticles in conventional heat transfer fluids, such as water or ethylene glycol, to enhance thermal conductivity. The corrugated pattern enhances the surface area that comes into contact with heat, allowing for more effective heat absorption. The significance is found in the enhanced effectiveness of heat transfer and absorption, along with a reduced pressure drop. A detailed comparative analysis on the variations in thermal performance of sinusoidal wavy corrugated plate heat exchangers at angles of 0°, 30°, 40°, and 50°, using MWCNT and CuO in water, has been conducted, addressing the literature gap where limited information exists. Flow rate of nanofluid was varied between 2 to 4 L/min and nanoparticle concentration from 0 to 0.09%. The impact of flowrate on convective heat transfer coefficient, pressure drop, and thermal hydraulic performance was studied. Findings indicate that CuO nanofluids are preferable for applications characterized by low flow rate (less than 2 L/min) and conduction dominance, such as cooling compact electronics or utilizing low-capacity heat exchangers, where increased particle concentration is acceptable. Conversely, MWCNT nanofluids are more appropriate for heat exchangers used on an industrial scale and in turbulent flow conditions, as they provide enhanced efficiency at reduced concentrations, which helps lower pumping power requirements and pressure.

Keywords: CuO nanofluid; Sinusoidal wavy corrugated plate heat exchanger; Heat transfer process; Pumping power.

1. INTRODUCTION

Nanofluids find applications in photovoltaic cells, solar energy systems, power plants and heat exchangers. Carbon nanotubes (CNTs) possess a high aspect ratio and thermal conductivity and hence are an excellent option as nanoparticles (Munkhbayar *et al*. 2013). Thermal conductivity improves by 15–160% when small amounts of CNTs are included in water, polyalphaolefin oil and ethane-1,2-diol (Kim *et al*. 2001; Choi *et al*. 2001; Xie *et al*. 2003; Liu *et al*. 2011). CNT nanofluids are shear-thinning fluids. The pressure drops of CNT nanofluids are similar to those of the base fluid due to the shear-thinning nature of CNT nanofluids in the turbulent regime (Ko *et al*. 2007). Higher heat transfer efficacy is observed with ethane-1,2-diol than water in streamlined flow at an identical Reynolds number for MWCNT nanofluid (Ruan and Jacobi, 2012). A 20% improvement in thermal conductivity was observed at 1 wt.% MWCNT–water nanofluid for 113 J/g optimal ultrasonic energy (Garg *et al*. 2009). MWCNT nanoparticles in a water–ethane-1,2-diol mixture augment thermal conductivity, diminish specific heat and increase viscosity ratio with temperature (Ganeshkumar *et al*. 2015). SWCNT nanofluids have greater thermal conductivity than MWCNT nanofluids, which amplify with volume concentration and temperature (Gohari *et al*. 2013). The base fluid has less thermal conductivity than nanofluids; aluminium–water nanofluid has less thermal conductivity compared to copper–water nanofluid (Abad and Zamzamian, 2013). Undecorated MWCNT-based nanofluids have less thermal conductivity than decorated ones (Farbod and Ahangarpour, 2016). MWCNT in viscoelastic fluids have greater thermal conductivity than base fluids, which rises with an increase in temperature and volume fraction. MWCNT in viscoelastic fluids behave as a non-Newtonian fluid (Li *et al.* 2013).

Nanofluids can be applied to solar energy systems (Wahab *et al.* 2019), though they have difficulties and restrictions (Shah and Ali, 2019). CuO/water nanofluids enhance the application of photovoltaic collectors (Michael and Iniyan, 2015). Solar energy conversion is improved with MWCNT (Chen *et al.* 2019). Exit temperature improved by 14.09% at 5 vol.% copper/water nanofluid in a vacuum tube solar collector (Yurddaş, 2020). CuO/water nanofluid enhances CPU cooling (Abbas *et al.* 2019). With an

increase of nanoparticle ratio and flow rate, the friction factor increased (Rashed *et al.* 2016). Optimum performance was realised at 1.5% of CuO/water nanofluid (Khairul *et al.* 2014; Nagaraju Dora *et al.* 2020). Hence, a detailed comparative analysis on the variations in thermal performance of sinusoidal wavy corrugated plate heat exchangers (SWCPHE) at angles of 0°, 30°, 40° and 50°, using MWCNT and CuO in water, has been conducted, addressing the literature gap where limited information exists.

2. MATERIALS AND METHODS

CuO nanoparticles and MWCNT in water are used as test fluids. Thermal conductivity (K), specific heat capacity (c) and density (ρ) of CuO nanoparticles and MWCNTs are 32.9 $Wm^{-1}K^{-1}$, 540 $JKg^{-1}K^{-1}$, 6400 Kgm^{-3} and 2000 $Wm^{-1}K^{-1}$, 733 $JKg^{-1}K^{-1}$, 40 Kgm^{-3} respectively. CuO nanoparticles were procured from Nano Research Lab while MWCNTs from Adnano Technologies Pvt Ltd. A customized SWCPHE was fabricated to conduct experiments (Fig. 1). Three plates of stainless steel were joined by welding so that two adjacent flow channels are formed. Upper flow conduit for nanofluid was 5 mm, and lower flow conduit for base fluid (Water) was 15 mm. The test rig configuration (Fig. 2) comprises of a tank for the test fluid, four test boxes having four different corrugation angles (0°, 30°, 40° and 50°; Fig. 3), a tank to collect test fluid or cold fluid or nanofluid, and a tank for hot water. Each test box comprises of three sinusoidal corrugated plates welded to create two horizontal channels to support the flow. The measurements of the SWCPHE are given in Table 1.



Fig. 1: SWCP and middle plate



Fig. 2: SWCPHE test rig

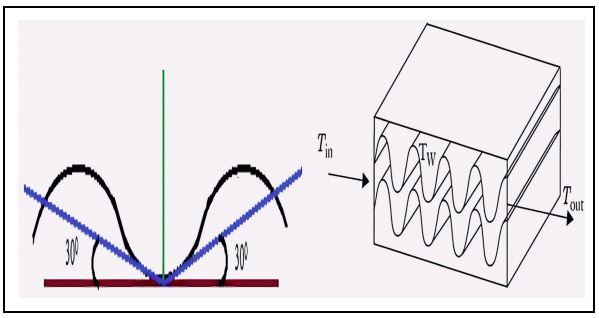


Fig. 3: SWCP and corrugated angle

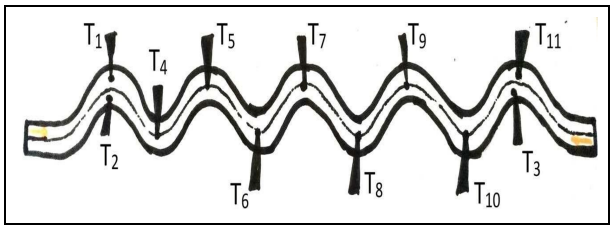


Fig. 4: SWCP with thermocouples

Table 1. Specifications of SWCPHE

S. No.	Specification	Unit
1	Plate length	30 cm
2	Plate width	10 cm
3	Plate spacing	0.5 cm
4	Plate angle	0, 30, 40 & 50°

Rotameters control the flow rate. Hot water was maintained at 70 °C and 3 L/min, while the flow rate of the test fluid varied from 2–4 L/min along with the variation of nanoparticle concentration (ϕ) at 0.01, 0.03, 0.05, 0.07 and 0.09%. Counter current flow pattern was used. Along the length of the top of the middle plate, seven thermocouples were fixed to measure temperatures (Fig. 4). Four thermocouples at the entry and exit of cold and hot fluids measure inlet and outlet temperatures of hot and cold fluids. A robust manometer was used to measure pressure drop. Volume fraction of nanoparticle in percentage was calculated by Equation 1 and Equation 2.

$$(\phi) = \frac{\text{volume}_{np}}{\text{volume}_{np} + \text{volume}_{water}} \quad \ldots (1)$$

$$= \frac{W_{np}/\rho_{np}}{W_{np}/\rho_{np} + W_{water}/\rho_{water}} \quad \ldots (2)$$

Thermal conductivity, Density, Specific heat were calculated by Equations (3), (4), (5), respectively.

$$K_{nf} = \frac{K_p + 2K_w + 2\phi(K_p - K_w)(1+2.5\phi)}{K_p + 2K_w - \phi(K_p - K_w)} K_w \quad \ldots (3)$$

$$\rho_{nf} = \emptyset\rho_p + (1 - \emptyset)\rho_w \quad \ldots . (4)$$

$$C_{nf} = \frac{[\phi(\rho_{np}\, C_{np}) + (1 - \phi)\,(\rho_w\, C_w)]}{\rho_{nf}} \quad \ldots (5)$$

K_{nf}, ρ_{nf}, C_{nf} are thermal conductivity, density, and specific heat of nanofluid, respectively.

Heat transfer was calculated by making an energy balance with the log-mean temperature difference. Average temperature, LMTD, heat transfer rate (Q), convective heat transfer coefficient (h) were calculated by Equations 6–9.

$$T_{avg} = \frac{T4+T5+T6+T7+T8+T9+T10}{7} \quad \ldots (6)$$

$$LMTD = \frac{(T_{avg} - T_{C,in}) - (T_{avg} - T_{C,out})}{\ln \frac{T_{avg} - T_{C,in}}{T_{avg} - T_{C,out}}} \quad \ldots (7)$$

$$Q = MFR.C_{nf}\,\Delta T_{nf} \quad \ldots (8)$$

$$Q = h\,A\,(LMTD) \quad \ldots (9)$$

MFR is mass flow rate of cold fluid.

Pictorial representation of test rig is illustrated in Fig. 5. Thermal hydraulic performance (THP) is the ratio of the heat transfer coefficient for the enhanced surface to that for a plain (flat) surface, adjusted for pressure drop or friction factor. It was calculated using Equation 10.

$$\frac{h_{cp}/h_{fp}}{\sqrt[3]{pd_{cp}/pd_{fp}}} \quad \ldots (10)$$

where h_{cp} is heat transfer coefficient of corrugated plate, h_{fp} is heat transfer coefficient of flat(0°) plate. pd_{cp}, pd_{fp} are pressure drop in corrugated plates and flat plate, respectively.

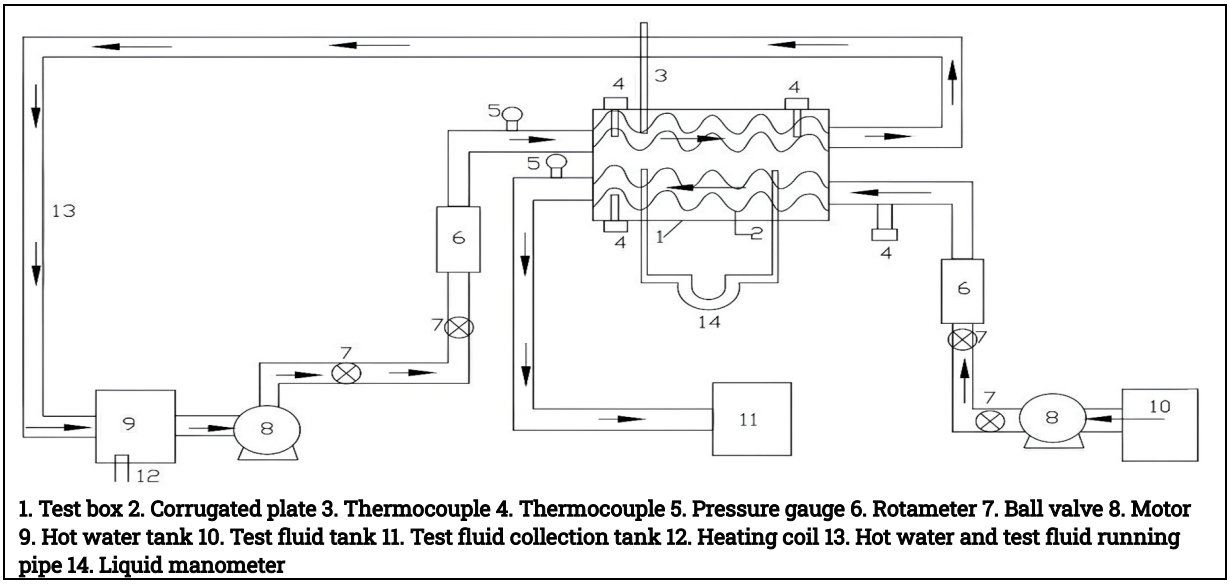


Fig. 5: Diagrammatic representation of experimental rig

SWCPs with 0°, 30°, 40° and 50° are shown in Fig. 6 - 9, respectively.

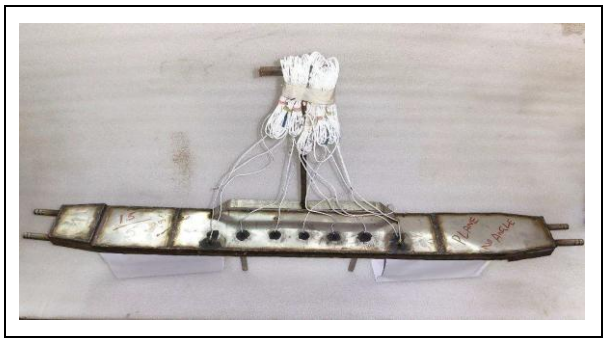


Fig. 6: Middle plate (0° corrugation angle)

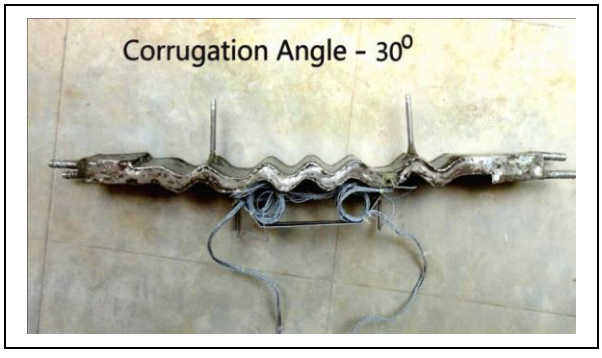


Fig. 7: 30° SWCP

3. RESULTS AND DISCUSSION

Fig. 10 - 12 show the variation of heat transfer coefficient (h) with nanoparticle concentration (ϕ) at 2, 3 and 4 L/min for CuO nanofluid. Due to low turbulence and high residence time, improvement in thermal conductivity (conduction) helps to boost h. With increasing ϕ, viscosity increases and, at low Reynolds number, secondary flows induced by geometry are dampened, due to which h declines or plateaus with ϕ.

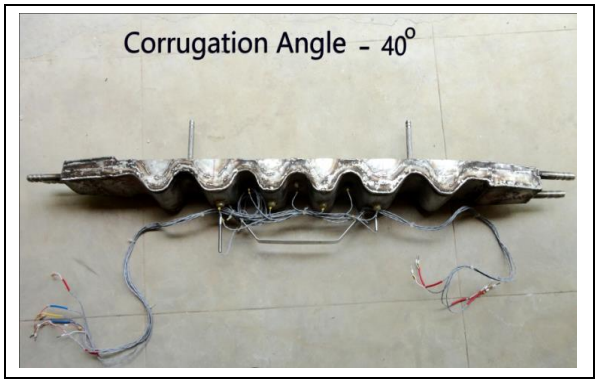


Fig. 8: 40° SWCP

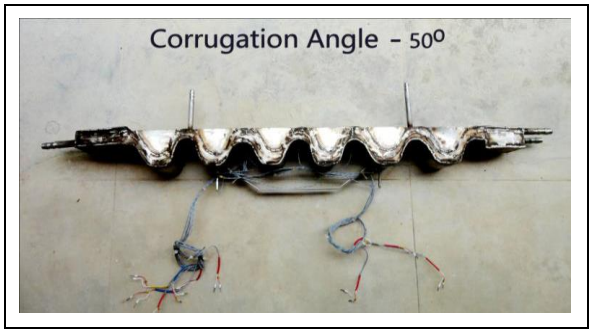


Fig. 9: 50° SWCP

The heat transfer coefficient increases with ϕ for all angles, with the 50° angle leading for all ϕ. Corrugations initiate secondary flow, which is complemented by improvement in conduction due to ϕ. Moderate Reynolds number, improved bulk thermal

conductivity and mixing due to corrugations increase h. An increase in h with ϕ, flow rate and corrugation angle is observed. A steep increase is observed for 40° and 50° after ϕ = 0.05. Higher Reynolds number combined with stronger mixing due to geometry translates bulk conductivity to higher h. The 0° angle (flat plate) does not have any secondary flows.

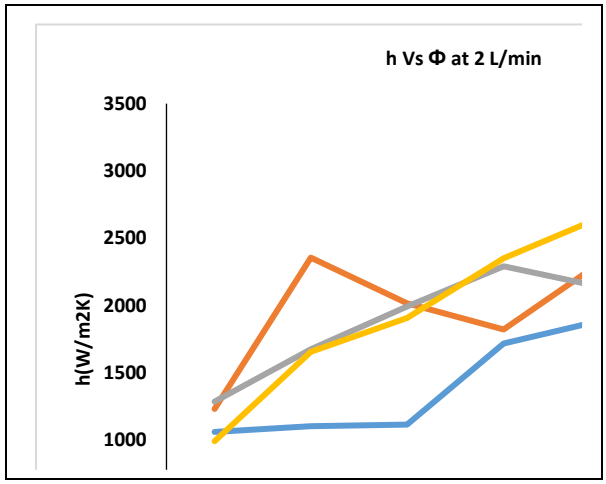


Fig. 10: Influence of ϕ on h at 2 L/min (CuO)

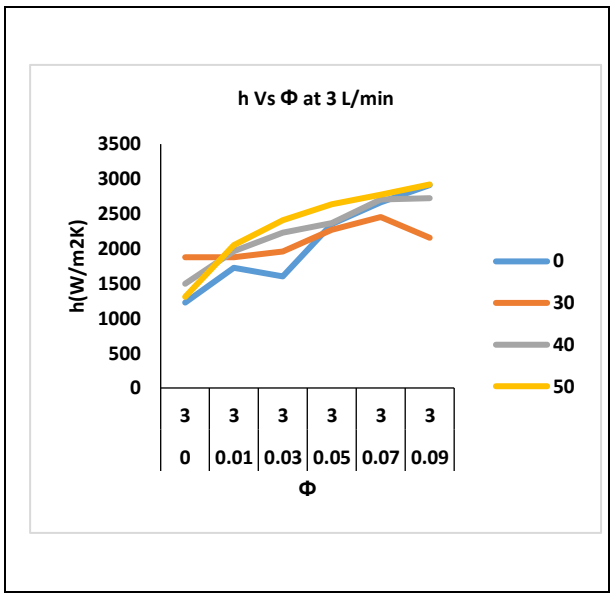


Fig. 11: Influence of ϕ on h at 3 L/min (CuO)

Fig. 13 - 15 represent h *vs.* ϕ for MWCNT nanofluid at 2, 3 and 4 L/min for 0°, 30°, 40° and 50° corrugated angles. The heat transfer coefficient rises up to ϕ = 0.01 and then plateaus or declines for all angles. At high ϕ, viscosity dampens turbulence and mixing, and at high ϕ MWCNTs agglomerate. The 50° angle gives the highest h for all angles. A peak is observed at ϕ = 0.01 and, with increase in ϕ, h plateaus. At moderate Reynolds number, corrugations create secondary flows and mixing, while viscous effects are prominent at increased ϕ. At ϕ = 0.01 the highest h is observed. At a sinusoidal angle of 50°, h is consistently high. At high Reynolds number, secondary flows and mixing created due to corrugations are effective. Higher angles give stronger mixing, secondary flows and disruption of the boundary layer, with increased h at small values of ϕ. Small conductivity gains translate into larger h. Plain geometry lacks secondary flows.

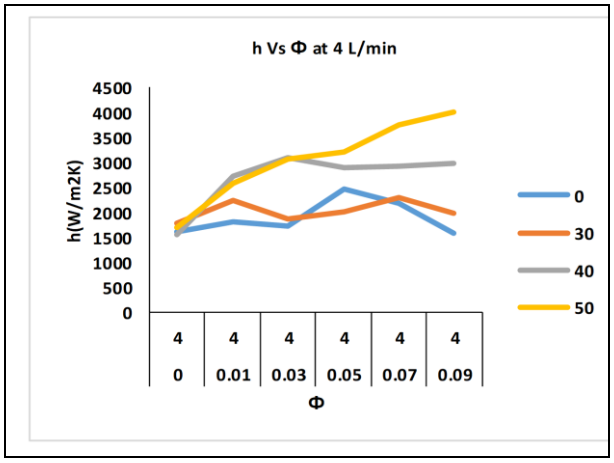


Fig. 12: Influence of ϕ on h at 4 L/min (CuO)

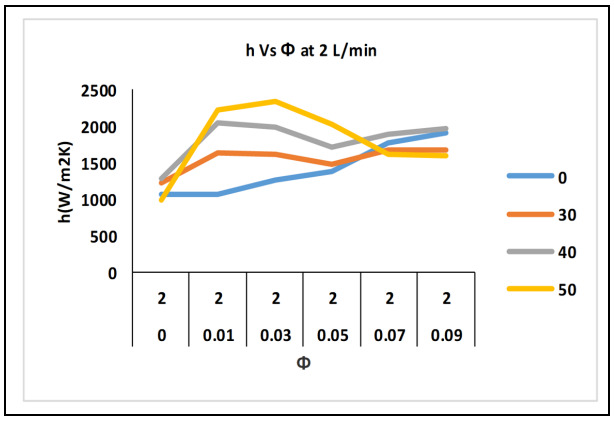


Fig. 13: Influence of ϕ on h at 2 L/min (MWCNT)

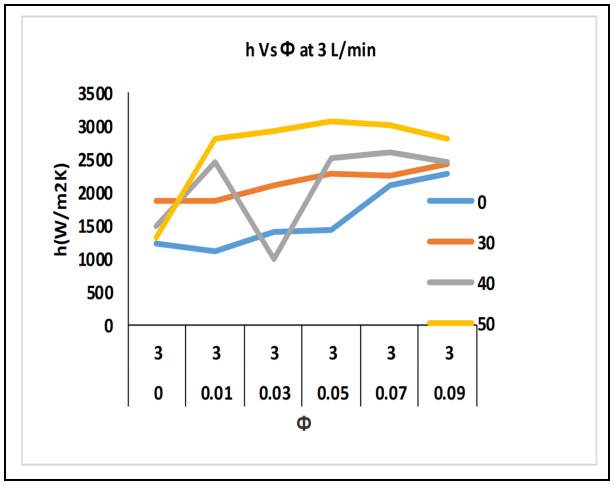


Fig. 14: Influence of ϕ on h at 3 L/min (MWCNT)

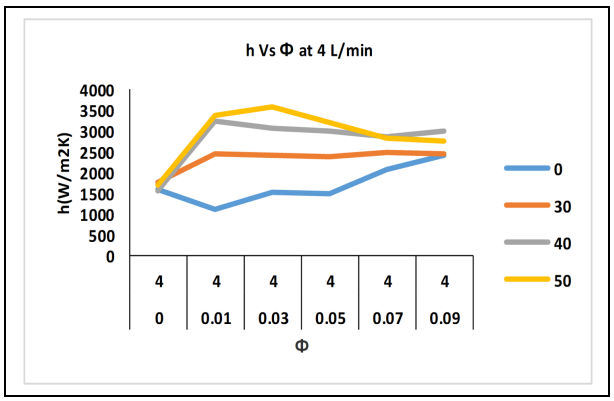


Fig. 15: Influence of ϕ on h at 4 L/min (MWCNT)

Fig. 16(a) and 16(b) show pressure drop vs. ϕ at 2, 3 and 4 L/min for the flat (0°) plate for MWCNT and CuO nanofluids, respectively. For the flat plate with MWCNT nanofluid, pressure drop increases with 2 and 3 L/min and with ϕ. However, at 4 L/min, anomalous behaviour is observed: pressure drop plummets from ϕ = 0 to ϕ = 0.01 and remains almost constant thereafter, with the least pressure drop observed at 4 L/min. For CuO, pressure drop increases with nanoparticle concentration and flow rate, with a steeper increase at 4 L/min.

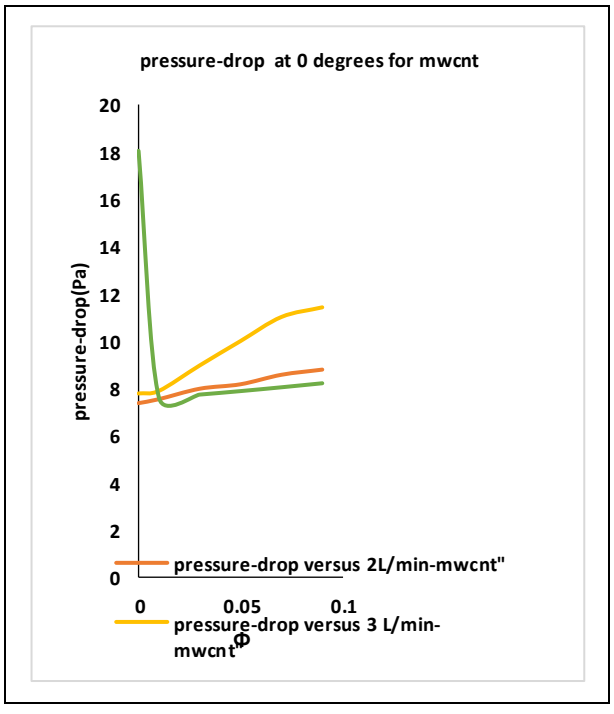


Fig. 16(a): Pressure drop at 2, 3, 4 L/min for 0° angle (MWCNT)

Fig. 17(a) and 17(b) show pressure drop vs. ϕ at 2, 3 and 4 L/min for the 30° angle for MWCNT and CuO nanofluids, respectively. Fig. 18(a) and 18(b) show pressure drop vs. ϕ at 2, 3 and 4 L/min for the 40° angle for MWCNT and CuO nanofluids, respectively. At 30° and 40°, pressure drop remains almost unchanged with nanoparticle concentration, and the maximum is observed at 4 L/min, increasing with angle for all concentrations for MWCNT. For CuO nanofluid, as angle increases from 0° to 30° to 40°, pressure drop rises with flow rate, and at 2 and 3 L/min, nanoparticle concentration has little effect; at 4 L/min, the rise is visible.

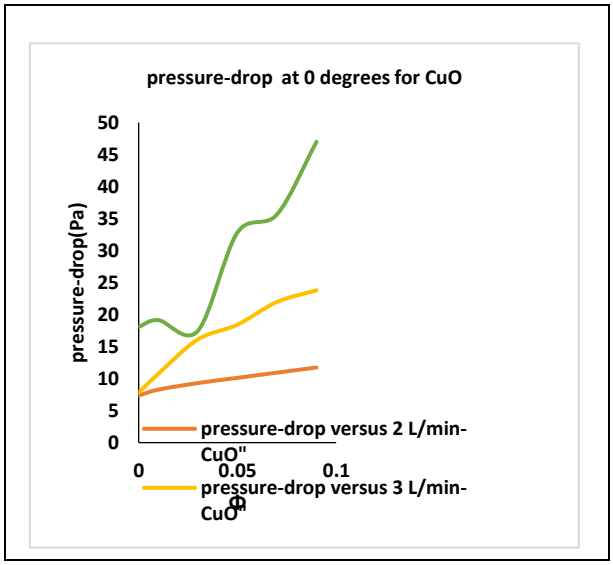


Fig. 16(b): Pressure drop at 2,3,4 L/min for 0° angle (CuO)

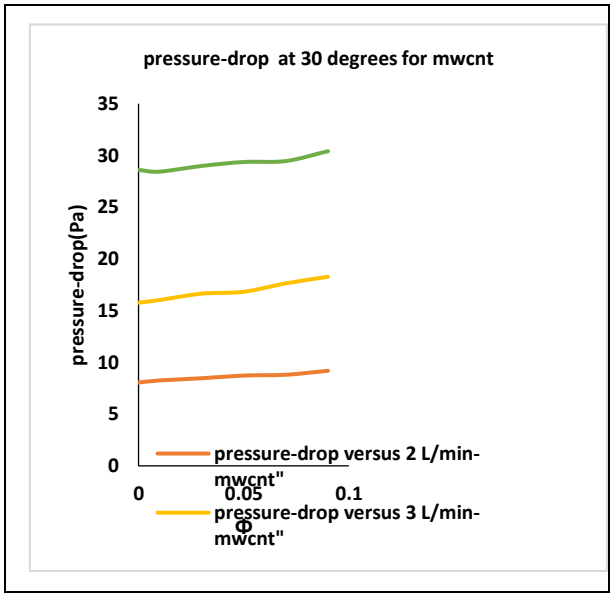


Fig. 17(a): Pressure drop at 2,3,4 L/min for 30° angle (MWCNT)

The same trend is observed for 50°, but pressure drop decreases compared to the 40° angle for all flow rates and ϕ for MWCNT. At 50° for CuO, pressure drop decreases compared to 40°, but increases with flow rate and nanoparticle concentration, with a steeper rise with concentration at 4 L/min, as shown in Fig. 19(a) and 19(b). It can be concluded that pressure drop increases

with nanoparticle concentration, plate angle and flow rate, and is higher for MWCNTs due to their high aspect ratio and tube entanglement.

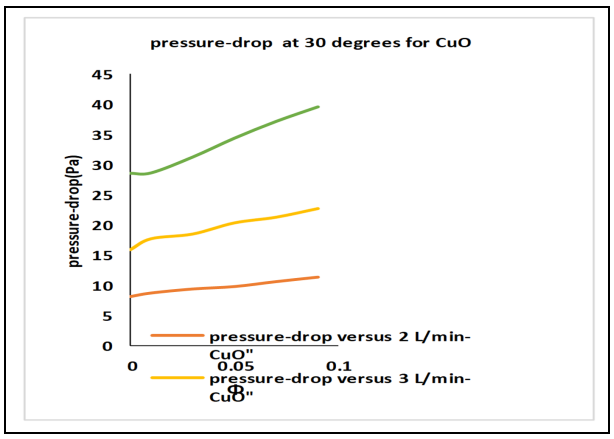


Fig. 17(b): Pressure drop at 2, 3, 4 L/min for 30° angle (CuO)

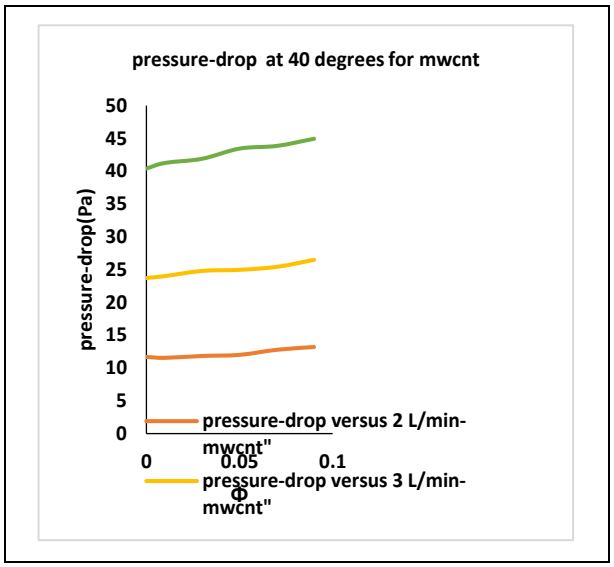


Fig. 18(a): Pressure drop at 2,3,4 L/min for 40° angle (MWCNT)

Thermal hydraulic performance evaluates the combined effect of convective heat transfer coefficient and pressure drop. Fig. 20–22 show the effect of ϕ on THP at 2, 3 and 4 L/min for CuO nanofluid. THP with CuO nanofluid increases with flow rate and ϕ for the 50° corrugated angle, while for the plain and 30° angles THP is independent of ϕ and remains at unity. Maximum THP is obtained for 50° at ϕ = 0.09. The increase in THP with ϕ is steep for 50° due to enhanced thermal conductivity and angle-induced turbulence, mixing and thermal residence time. Higher THP is observed for higher corrugation angle, high particle ratio(ϕ) and low or medium flow rates (laminar flow with strong mixing due to corrugation angle).

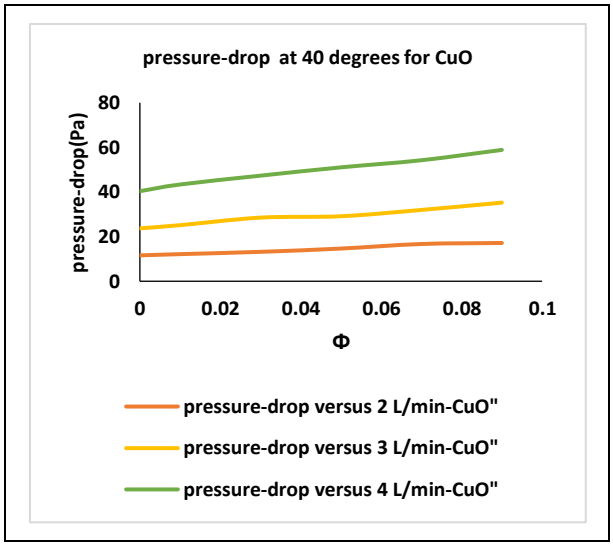


Fig. 18(b): Pressure drop at 2, 3, 4 L/min for 40° angle (CuO)

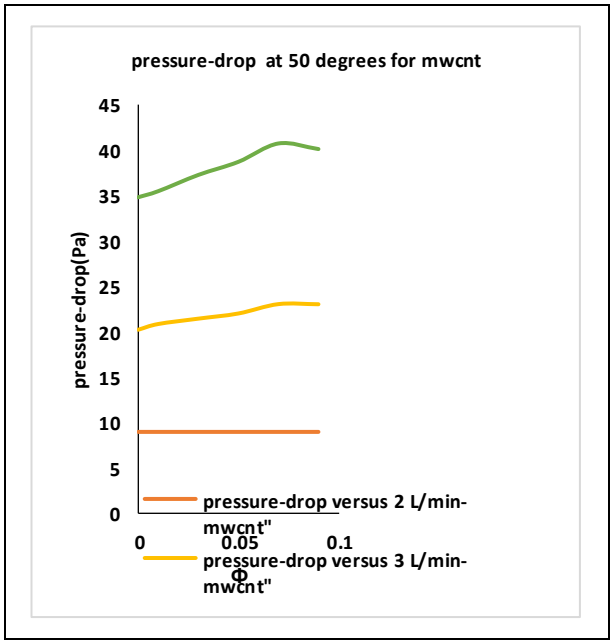


Fig. 19(a): Pressure drop at 50° angle (MWCNT)

Fig. 23–25 show the effect of ϕ on THP at 2, 3 and 4 L/min for MWCNT nanofluid. A declining trend in THP is observed after ϕ = 0.01 for all flow rates and angles. The highest THP is observed at ϕ = 0.01 for 50°. Low angles are independent of ϕ, while the 50° angle shows a steep rise up to ϕ = 0.01 and plateaus from there on. Because of the higher thermal conductivity and aspect ratio compared to CuO, THP increases with nanoparticle concentration up to ϕ = 0.01 and declines thereafter due to viscosity. The maximum is observed for 50° at ϕ = 0.01.

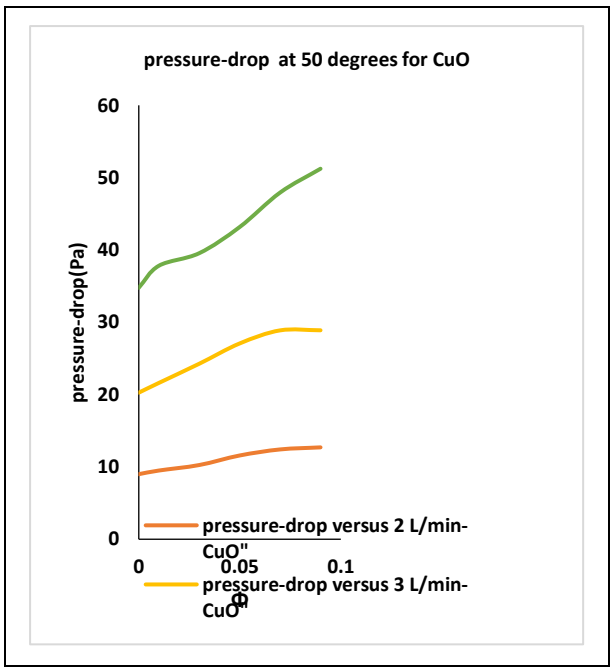


Fig. 19(b): Pressure drop at 2,3,4 L/min for 50° angle (CuO)

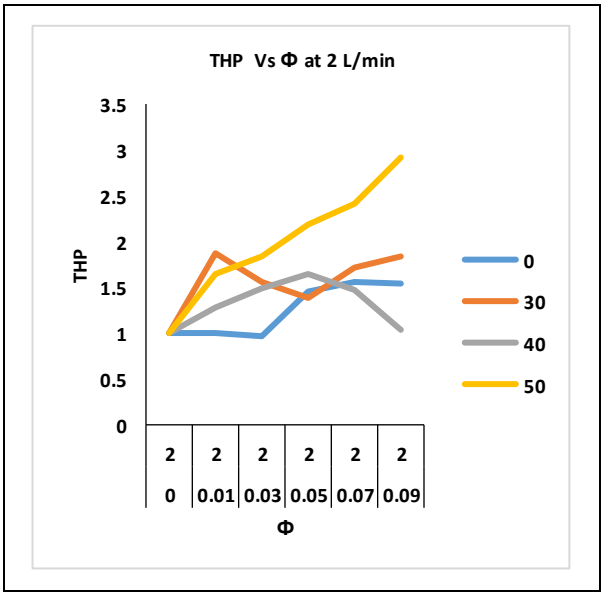


Fig. 20: Effect of ϕ on THP at 2 L/min (CuO)

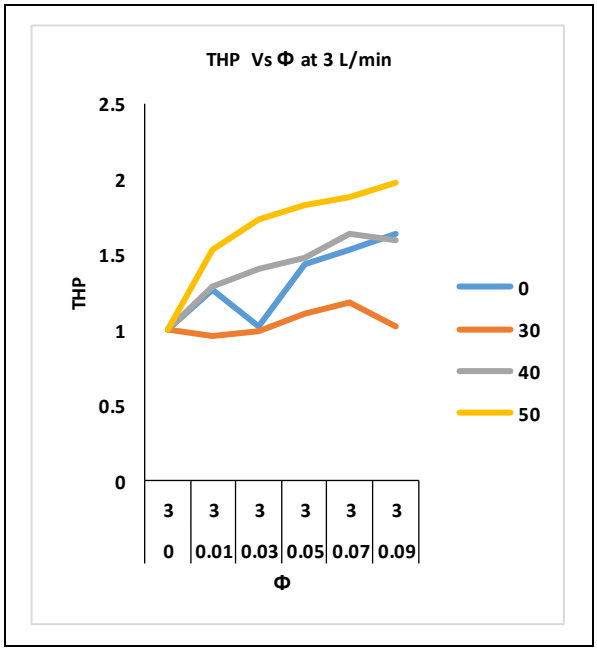


Fig. 21: Effect of ϕ on THP at 3 L/min (CuO)

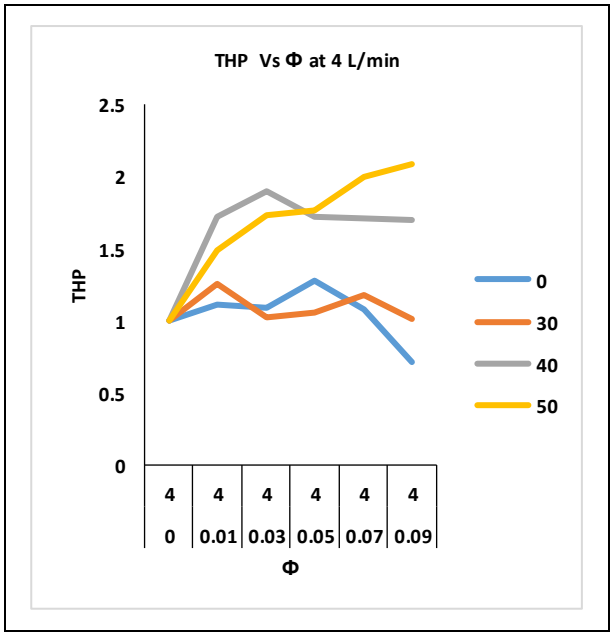


Fig. 22: Effect of ϕ on THP at 4 L/min (CuO)

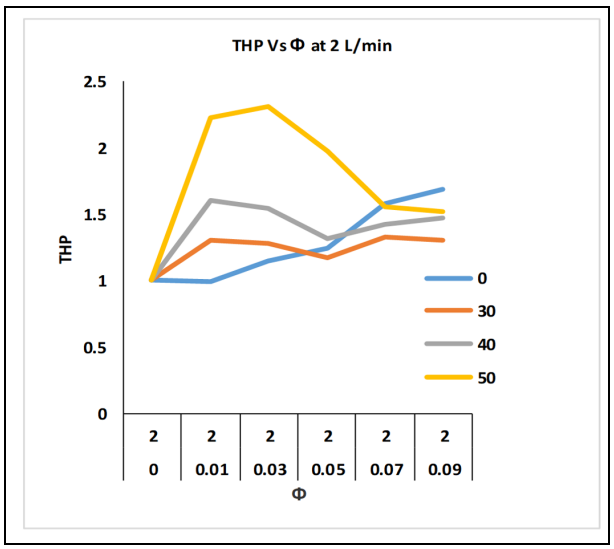


Fig. 23: Effect of ϕ on THP at 2 L/min (MWCNT)

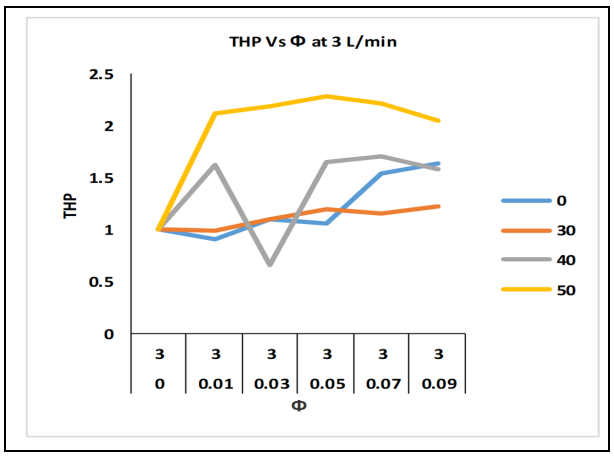


Fig. 24: Effect of ϕ on THP at 3 L/min (MWCNT)

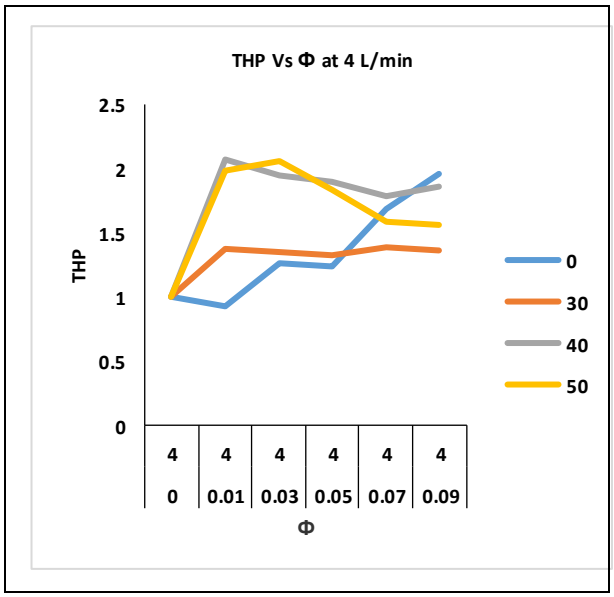


Fig. 25: Effect of ϕ on THP at 4 L/min (MWCNT)

4. CONCLUSIONS

The comparative study of CuO/water and MWCNT/water nanofluids shows distinct thermal hydraulic performance trends depending on flow conditions and nanoparticle concentration. CuO nanofluids exhibited maximum THP enhancement at low flow rates (2 L/min) and higher particle concentrations ($\phi \geq 0.07–0.09$), where conduction and Brownian motion effects dominate. However, at higher flow rates, the improvement was marginal due to turbulence-driven heat transfer and viscosity penalties. In contrast, MWCNT nanofluids achieved superior THP at moderate concentrations ($\phi = 0.01–0.05$) and higher flow rates (3–4 L/min), particularly at larger corrugation angles (40°–50°). This is attributed to the exceptionally high thermal conductivity and aspect ratio of MWCNTs, which form conductive networks that synergize with turbulence-induced mixing.

From a practical perspective, CuO nanofluids are more suitable for low-flow(<2 L/min), conduction-dominated applications such as compact electronics cooling or low-capacity heat exchangers, where high particle loading can be tolerated. MWCNT nanofluids, on the other hand, are better suited for industrial scale and turbulent flow heat exchangers, as they deliver higher efficiency at lower concentrations(ϕ=0.01%), minimizing pumping power and pressure drop penalties. Overall, CuO is more effective at low flow rates and higher concentrations, while MWCNT is more effective at higher flow rates and moderate concentrations in wavy plate heat exchangers.

ACKNOWLEDGEMENT

The authors express sincere gratitude for the support given by Chaitanya Bharathi Institute of Technology, Telangana, for the conduction of experiments.

CONFLICTS OF INTEREST

The authors declare that there is no conflict of interest.

COPYRIGHT

This article is an open-access article distributed under the terms and conditions of the Creative Commons Attribution (CC BY) license (http://creativecommons.org/licenses/by/4.0/)

REFERENCES

Abad, M. T. J. and Zamzamian, A., Thermal conductivity of Cu and Al-water nanofluids, *Int. J. Eng.,* 26(8), 821–828(2013). https://doi.org/10.5829/IDOSI.IJE.2013.26.08B.03

Abbas, N., Awan, M. B., Amer, M., Ammer, S. M., Sajjad, U., Ali, H. M., Zahra, N., Hussain, M., Badshah, M. A. and Jafry, A. T., Applications of nanofluids in photovoltaic thermal systems: a review of recent advances, *Physica A.,* 536, 122513(2019). https://doi.org/10.1016/j.physa.2019.122513

Chen, W., Zou, C. and Li, X., Application of large-scale prepared MWCNTs nanofluids in a solar energy system as volumetric solar absorber, *Sol. Energy Mater. Sol. Cells.,* 200, 109931(2019). https://doi.org/10.1016/j.solmat.2019.109931

Choi, S. U. S., Zhang, Z. G., Yu, W., Lockwood, F. E. and Grulke, E. A., Anomalous thermal conductivity enhancement in nanotube suspensions, *Appl. Phys. Lett.,* 79(14), 2252–2254(2001). https://doi.org/10.1063/1.1408272

Dora, N., Mendu, S. S. and Raju, B. H. L., Comparative study of conjugate heat transfer characteristics in chevron corrugated plate heat exchanger using CuO nanocoolant, *Arabian J. Sci. Eng.,* 45(11), 8955–8967(2020). Citation not found https://doi.org/10.1007/s13369-020-04631-2

Farbod, M. and Ahangarpour, A., Improved thermal conductivity of Ag-decorated carbon nanotubes water-based nanofluids, *Phys. Lett. A.*, 380(48), 4044–4048(2016). https://doi.org/10.1016/j.physleta.2016.10.014

Ganeshkumar, J., Kathirkaman, D., Raja, K., Kumaresan, V. and Velraj, R., Experimental study on density, thermal conductivity, specific heat and viscosity of water–ethylene glycol mixture dispersed with carbon nanotubes, *Therm. Sci.,* 21(1 Part A), 255-265(2015). https://doi.org/10.2298/TSCI141015028G

Garg, P., Alvarado, J. L., Marsh, C., Carlson, T. A., Kessler, D. A. and Annamalai, K., An experimental study on the effect of ultrasonication on viscosity and heat transfer performance of multiwall carbon nanotube-based aqueous nanofluids, *Int. J. Heat Mass Transfer.,* 52(21-22), 5090–5101(2009). https://doi.org/10.1016/j.ijheatmasstransfer.2009.04.029

Khairul, M. A., Alim, M. A., Mahbubal, I. M., Saidur, R., Hepbasli, A. and Hossain, A., Heat transfer performance and exergy analyses of a corrugated plate heat exchanger using metal oxide nanofluids, *Int. Commun. Heat Mass Transfer.,* 50, 8-14(2014). https://doi.org/10.1016/j.icheatmasstransfer.2013.11.006

Kim, P., Shi, L., Majumdar, A. and McEuen, P., Thermal transport measurements of individual multiwalled nanotubes, *Phys. Rev. Lett.,* 87(21), 215502(2001). https://doi.org/10.1103/PhysRevLett.87.215502

Ko, G. H., Heo, K., Lee, K., Kim, D. S., Kim, C., Sohn, Y. and Choi, M., An experimental study on the pressure drop of nanofluids containing carbon nanotubes in a horizontal tube, *Int. J. Heat Mass Transfer.,* 50(23-24), 4749–4753(2007). https://doi.org/10.1016/j.ijheatmasstransfer.2007.03.029

Li, F. C., Yang, J. C., Zhou, W. W., He, Y. R., Huang, Y. M. and Jiang, B. C., Experimental study on the characteristics of thermal conductivity and shear viscosity of viscoelastic-fluid-based nanofluids containing multiwalled carbon nanotubes, *Thermochimica Acta.,* 556, 47–53(2013). https://doi.org/10.1016/j.tca.2013.01.023

Liu, M., Lin, M. C. and Wang, C., Enhancements of thermal conductivities with Cu, CuO, and carbon nanotube nanofluids and application of MWNT/water nanofluid on a water chiller system, *Nanoscale Res. Lett.,* 6(1), 297(2011). https://doi.org/10.1186/1556-276X-6-297

Tajik Jamal Abad M,Rashidi A.M.,Gohari M., An experimental study on the thermal conductivity of carbon nanotubes/oil(TECHNICAL NOTE)', *Int. J. Eng.,* 27(3), 411–416(2013). https://doi.org/10.5829/idosi.ije.2014.27.03c.08

Michael, J. J. and Iniyan, S., Performance analysis of a copper sheet laminated photovoltaic thermal collector using copper oxide-water nanofluid, *Sol. Energy.,* 119, 439–451(2015). https://doi.org/10.1016/j.solener.2015.06.028

Munkhbayar, B., Tanshen, M. R., Jeoun, J., Chung, H. and Jeong, H., Surfactant-free dispersion of silver nanoparticles into MWCNT-aqueous nanofluids prepared by one-step technique and their thermal characteristics, *Ceram. Int..,* 39(6), 6415–6425(2013). https://doi.org/10.1016/j.ceramint.2013.01.069

Rashed, M. H. A., Dzido, G., Korpys, M., Smolka, J. and Wojcik, J., Investigation on the CPU nanofluid cooling, *Microelectron. Reliab.,* 63, 159–165(2016). https://doi.org/10.1016/j.microrel.2016.06.016

Ruan, B. and Jacobi, A. M., Heat transfer characteristics of multiwall carbon nanotube suspensions (MWCNT nanofluids) in intertube falling-film flow, *Int. J. Heat Mass Transfer.,* 55(11), 3186–3195(2012). https://doi.org/10.1016/j.ijheatmasstransfer.2012.02.051

Shah, T. R. and Ali, H. M., Applications of hybrid nanofluids in solar energy, practical limitations and challenges: a critical review, *Sol. Energy.,* 183, 173–203(2019). https://doi.org/10.1016/j.solener.2019.03.012

Wahab, A., Hassan, A., Qasim, M. A., Ali, H. M., Babar, H. and Sajid, M. U., Solar energy systems—potential of nanofluids, *J. Mol. Liq.,* 289, 111049(2019). https://doi.org/10.1016/j.molliq.2019.111049

Xie, H., Lee, H., Youn, W. and Choi, M., Nanofluids containing multiwalled carbon nanotubes and their enhanced thermal conductivities, *J. Appl. Phys.,* 94(8), 4967–4971(2003). https://doi.org/10.1063/1.1613374

Yurddaş, A., Optimization and thermal performance of evacuated tube solar collector with various nanofluids, *Int. J. Heat Mass Transfer.,* 152, 119496(2020). https://doi.org/10.1016/j.ijheatmasstransfer.2020.1194